THERMODYNAMIC STABILITY OF ACTINIDE PYROCHLORE MINERALS IN DEEP GEOLOGIC REPOSITORY ENVIRONMENTS

Yifeng Wang*, Huifang Xu**
* Sandia National Laboratories, 4100 National Parks Highway, Carlsbad, New Mexico 88220. E-mail: ywang@sandia.gov
** Department of Earth and Planetary Sciences, The University of New Mexico, Albuquerque, New Mexico 87131. E-mail: hfxu@unm.edu

ABSTRACT

Crystalline phases of pyrochlore (e.g., $CaPuTi_2O_7$, $CaUTi_2O_7$) have been proposed as a durable ceramic waste form for disposal of high level radioactive wastes including surplus weapons-usable plutonium. In this paper, we use a linear free energy relationship to predict the Gibbs free energies of formation of pyrochlore phases ($CaMTi_2O_7$). The Pu-pyrochlore phase is predicted to be stable with respect to PuO_2, $CaTiO_3$, and TiO_2 at room temperatures. Pu-pyrochlore is expected to be stable in a geologic repository where silica and carbonate components are absent or limited. We suggest that a repository in a salt formation be an ideal environment for disposal of high level, pyrochlore-based ceramic wastes. In such environment, adding CaO as a backfill will make pyrochlore minerals thermodynamically stable and therefore effectively prevent actinide release from these mineral phases.

INTRODUCTION

Crystalline phases of pyrochlore (e.g., $CaPuTi_2O_7$, $CaUTi_2O_7$) have been proposed as a durable ceramic waste form for disposal of high level radioactive wastes including surplus weapons-usable plutonium [1, 2]. Pyrochlore phases typically have a derivative fluorite structure and have a stoichiometry of $CaMTi_2O_7$, where M represents tetravalent cations such as Zr, Hf, U, Pu and other actinides. The existence of large polyhedra (with coordination numbers ranging from 7 to 8) in mineral structure allows pyrochlore phases to accommodate a wide range of radionuclides (e.g., Pu, U, Ba, etc.) as well as neutron poisons (e.g., Hf, Gd) [3].

Since most of the existing work on pyrochlore minerals has been focused on fabrication, structural characterization and leaching tests, the thermodynamic data of these mineral phases are still lacking. In this paper, we will use a linear free energy relationship to predict the Gibbs free energies of formation for various pyrochlore phases. Based on the predicted Gibbs free energies, the stability of actinide pyrochlore minerals in deep geologic repository environments will be discussed.

LINEAR FREE ENERGY RELATIONSHIP

Sverjensky and Molling have developed a linear free energy relationship that correlates the Gibbs free energies of formation of an isostructural family of inorganic

DISCLAIMER

solids with chemical properties of aqueous free cations [4]. This free energy relationship has been successfully applied to a wide variety of mineral phases [4, 5, 6, 7]. The linear free energy relationship for an isotructural family of minerals can be expressed as [4, 5]:

$$\Delta G^0_{f,MX} = a_{MX}\,\Delta G^0_{n,M^{Z+}} + b_{MX} + \beta_{MX}\, r_{M^{Z+}} . \qquad (1)$$

where the coefficients a_{MX}, b_{MX}, and β_{MX} characterize a particular structural family of minerals MX; $r_{M^{Z+}}$ is the ionic radius of cation M^{Z+}; the parameter $\Delta G^0_{f,MX}$ is the standard Gibbs free energies of formation of solid MX; and the parameter $\Delta G^0_{n,M^{Z+}}$ is the standard non-solvation energy from a radius-based correction to the standard Gibbs free energy of formation of the aqueous tetravalent cation M^{4+} [4]. The parameter $\Delta G^0_{n,M^{Z+}}$ can be calculated by:

$$\Delta G^0_{n,M^{Z+}} = \Delta G^0_{f,M^{Z+}} - \Delta G^0_{s,M^{Z+}} \qquad (2)$$

where $\Delta G^0_{s,M^{Z+}}$ is the standard Gibbs free energy of solvation of cation M^{Z+}, which can be calculated from conventional Born solvation coefficients [4].

The terms of $\Delta G^0_{n,M^{Z+}}$ and $r_{M^{Z+}}$ are known for free metal cations. The coefficients of a_{MX}, b_{MX}, and β_{MX} can be determined by fitting the equation to limited experimental data of $\Delta G^0_{f,MX}$ in an isostructural family of solids. The obtained equation can be then used to predict the unknown $\Delta G^0_{f,MX}$ for other solids within the same family.

PREDICTION OF GIBBS FREE ENERGIES OF FORMATION OF ACTINIDE PYROCHLORE MINERALS

Since no $\Delta G^0_{f,MX}$ data are currently available for pyrochlore phases, Equation (1) can not be directly applied to these mineral phases. Instead, the coefficients in Equation (1) for pyrochlore phases are extrapolated from zirconolite data. For the isostructural family of $CaMTi_2O_7$ with a zirconolite structure, the Gibbs free energies of formation have been determined for the $CaZrTi_2O_7$ and $CaHfTi_2O_7$ phases [8, 9]. In order to apply the above linear free energy relationship, the coefficient a_{MX} or β_{MX} needs to be estimated independently. The coefficient β_{MX} is related to the effect of nearest neighbors or coordination number (CN) of cation [4]. In polymorphs, a structure family with a small CN (e.g., CN = 6 in calcite structure family) has a higher value of β_{MX} than a family with a big CN (e.g., CN = 9 in aragonite structure family) does [4]. The value of β_{MX} for the MO_2 family with a fluorite structure (CN of M atom is 8) is 32.0 (kcal/mole·Å) (Table 1). The value of β_{MX} for the $MSiO_4$ family with a zircon structure (CN of M atom is 7) is 64.83 (kcal/mole·Å) [5. 6]. As a first-order approximation, we use β_{MX} value of 65 (kcal/mole·Å) for the zirconolite family (CN = 7). Using the Gibbs free energies of

formation of $CaZrTi_2O_7$ and $CaHfTi_2O_7$ phases [8, 9], the coefficients of a_{MX} and b_{MX} for zirconolite family can be calculated to be 0.5717 and -1024.06 kcal/mole, respectively.

Based on the results from other oxide and silicate families, the coefficient a_{MX} seems only related to the stoichiometry of solids [4]. Values of the coefficient a_{MX} are very close for all polymorphs [4]. Therefore, the a_{MX} value of 0.5717 is applied to pyrochlore phases. Similarly, we apply the β_{MvX} value of 32 (kcal/mole·Å) obtained for the MO_2 family with fluorite structure (CN = 8) to the pyrochlore family. The main difference between zirconolite and pyrochlore with the same stoichiometry of $CaMTi_2O_7$ is the coordination number of Zr. The coordination number of M atoms in the zirconolite structure and pyrochlore structure are 7 and 8, respectively. The difference in Gibbs free energies between calcite ($CaCO_3$) and aragonite polymorphs is about 0.2 (kcal/mole) [4]. The difference in Gibbs free energies between Al-Si ordered low-albite (CN of Na atom is 7) and Al-Si disordered high-albite (CN of Na atom is 9) polymorphs is about 2.0 (kcal/mole) [10]. However, the contribution from Al-Si odering in tetrahedral sites that can be calculated from the Gibbs free energies of formation of Al-Si ordered microcline and Al-Si disordered sanidine is about 1.6 (kcal/mole) [10]. Thus, the free energy contribution from the difference in coordination number of low-albite and high albite is about 0.4 (kcal/mole). Therefore, we postulate that the Gibbs free energy difference between the zirconolite and pyrochlore structures is within the range of 0.2 — 0.4 kcal/mole. It is proposed here that the Gibbs free energy of formation for Zr-pyrochlore ($CaZrTi_2O_7$) is about 0.3 (kcal/mole) higher than that of Zr-zirconolite ($CaZrTi_2O_7$). The coefficient b_{MvX} for pyrochlore phases is thus -997.67 (kcal/mole). The predicted standard Gibbs free energies of formation for other phases in the pyrochlore family with a stoichiometry of $CaM^{4+}Ti_2O_7$ are listed in Table 1.

THERMODYNAMIC STABILITY OF PYROCHLORE MINERALS IN DEEP GEOLOGIC REPOSITORY ENVIRONMENTS

Based on the predicted Gibbs free energies of formation of pyrochlore and Gibbs free energies of formation of perovskite and rutile [11], we can calculate the Gibbs free energy change of the following reaction ($\delta\Delta G_{rxt}$) of the reaction at a room temperature:

$$\underset{}{MO_2} + \underset{\text{perovskite}}{CaTiO_3} + \underset{\text{rutile}}{TiO_2} = \underset{\text{pyrochlore}}{CaMTi_2O_7}. \qquad (3)$$

The calculated Gibbs free energy changes ($\delta\Delta G_{rxt}$) are listed in Table 1. The Ce-pyrochlore has been synthesized by sintering oxides of CeO_2, $CaTiO_3$, and TiO_2 [12, 13]. As the annealing temperature decreases (from 1300 °C to 1140 °C), the proportions of Ce-pyrochlore increases by consuming oxides of CeO_2 and $CaTiO_3$ phases [13]. This experimental observation is consistent with our prediction of the negative Gibbs free energy change across reaction (3) for Ce-pyrochlore. In contrast, Th-pyrochlore phase will be unstable with respect to ThO_2, $CaTiO_3$, and TiO_2, To our knowledge, no

successful synthesis of Th-pyrochlore phase has been reported. It can be seen from Table 1 that the Gibbs free energy change in reaction (3) for Pu-pyrochlore (3) is more negative than that of Ce-pyrochlore (Table 1), indicating that the synthesis of Pu-pyrochlore from oxides is thermodynamically feasible.

Table 1. Ionic radii, thermodynamic data for aqueous cations, and predicted standard Gibbs free energies of formation (kcal/mole) [5]

M^{4+}	r_M4+ (Å)	$\Delta G_s M^{4+}$	$\Delta G_f M^{4+}$	$\Delta G_n M^{4+}$	MO_2 (Exper.)	MO_2 (Calculated)	ΔG_f Pyrochlore $CaMTi_2O_4$	$\delta\Delta G_{rxt}$ Reaction (3)
Zr	0.79	-373.11	-141.00	232.11	-249.23	-249.21	-839.70	-1.67
Hf	0.78	-374.41	-156.80	217.61	-260.09	-259.24	-848.30	-0.24
Ce	0.94	-354.23	-120.40	233.79	-244.40	-243.28	-833.93	-1.83
Th	1.02	-344.65	-168.50	176.13	-279.34	-279.35	-864.34	3.83
U	0.97	-350.60	-124.40	226.20	-246.62	-247.40	-837.31	-1.09
Np	0.95	-353.02	-120.20	232.82	-244.22	-243.61	-834.17	-1.74
Pu	0.93	-355.45	-115.00	240.49	-238.53	-239.11	-830.42	-2.49
Am	0.92	-356.68	-89.20	267.48	-220.72	-221.35	-815.31	-5.14
Po	1.10	-339.98	70.00	409.98		-121.39	-729.36	-11.54

The negative Gibbs free energy change in reaction (3) predicted for Pu-pyrochlore implies that this mineral phase is stable with respect to PuO_2, $CaTiO_3$, and TiO_2 at a room temperature. A reaction-path calculation using computer code EQ3/6 [14] shows that PuO_2 and TiO_2 are both stable in a Yucca Mountain environment. Considering that the Yucca Mountain repository is relatively oxic, we expect PuO_2 to be stable in most deep repository environments. Therefore, out of three minerals in the left side of reaction (3), at least two of them are stable. The stability of Pu-pyrochlore thus depends on the stability of perovskite ($CaTiO_3$).

The stability of perovskite ($CaTiO_3$) is controlled by the fugacity of CO_2 and the activity of silica. In the presence of silica or CO_2, perovskite ($CaTiO_3$) is unstable in a low temperature environment [15], because of the following reactions:

$$\underset{\text{perovskite}}{CaTiO_3} + H_4SiO_4(aq) = \underset{\text{sphene}}{CaTiSiO_5} + 2H_2O \qquad \log K = 8.9 \qquad (4)$$

$$\underset{\text{perovskite}}{CaTiO_3} + CO_2(g) = \underset{\text{calcite}}{CaCO_3} + \underset{\text{rutile}}{TiO_2} \qquad \log K = 8.5 \qquad (5)$$

where K is the equilibrium constant of the reaction and is calculated using the data from [11]. However, in the absence of both silica and CO_2, $CaTiO_3$ will be stable in an aqueous solution, because the following reaction is thermodynamically not favorable:

$$\underset{\text{perovskite}}{CaTiO_3} + H_2O = \underset{\text{portlandite}}{Ca(OH)_2} + TiO_2 \qquad \log K = -4.3 \qquad (6)$$

Consequently, Pu-pyrochlore will also become stable. Based on this argument, we suggest that a repository in a salt formation be an ideal environment for disposal of high level, pyrochlore-based ceramic wastes. The stability of pyrochlore and perovskite in this environment can be further ensured by adding CaO as a backifll. CaO will sequester any carbonate originally present in groundwater through reaction:

$$\underset{\substack{\text{Bruicte} \\ \text{(hydrated CaO)}}}{Ca(OH)_2} + CO_2 = \underset{\text{calcite}}{CaCO_3} \qquad \log K = 12.8 \qquad (7)$$

and, therefore, will keep both pyrochlore and perovskite minerals thermodynamically stable in the repository.

Even for a repository located in a silicate rock, depending on groundwater flow rates, silica and carbonate may become depleted in the near field due to chemical reactions, and then pyrochlore and perovskite may be still able to approach a stable state. In short, to assess the performance of pyrochlore ceramic waste, silica and carbonate concentrations in the near field must be carefully evaluated.

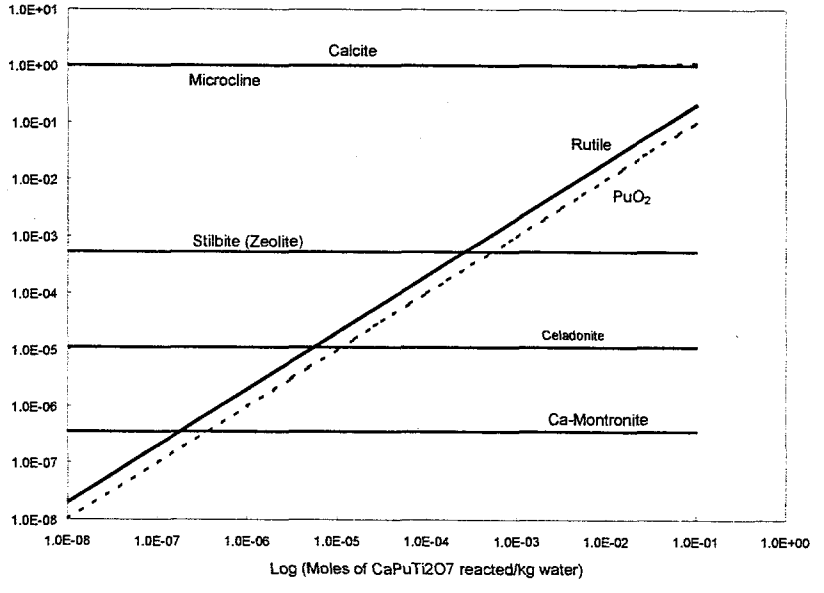

Figure 1. Reaction path calculation for Pu-pyrochlore dissolution in a Yucca Mountain repository environment. The fugacities of oxygen and carbon dioxide are maintained at 3.3×10^{-30} atm and 5.0×10^{-3} atm, respectively.

CONCLUSIONS

A linear free energy relationship has been used to predict the Gibbs free energies of formation of pyrochlore phases ($CaMTi_2O_7$). The coefficients in Equation (1) for pyrochlore phases are estimated to be: $a_{MX} = 0.5717$, $b_{MX} = -997.67$ (kcal/mole), and $\beta_{MX} = 32$ (kcal/mole·Å). The Pu-pyrochlore phase is predicted to be stable with respect to PuO_2, $CaTiO_3$, and TiO_2 at room temperatures. Pu-pyrochlore is expected to be stable in a geologic repository where silica and carbonate components are absent or limited. A repository in a salt formation is proposed as an ideal environment for disposal of high level, pyrochlore-based ceramic wastes. In such environment, adding CaO as a backfill will make pyrochlore minerals thermodynamically stable and therefore effectively prevent actinide release from these mineral phases.

ACKNOWLEDGMENTS

Sandia is a multiprogram operated by Sandia Corporation, a Lockheed Martin Company, for the United States Department of Energy under Contract DE-AC04-94AL8500.

REFERENCES

1. R.G. Dosch, T.J. Headley, C.J. Northrup, and P.F. Hlava, Sandia National Laboratories, Albuquerque, NM, Report SAND82-2980 (1983).
2. A.E. Ringwood, S.E. Kesson, K.D. Reeve, D.M. Levins, and E.J. Ramm, Synroc, In *Radioactive Waste Forms for the Future*, edited by W. Lutze and R.C. Ewing, (North-Holland, Amsterdam, 1988), p. 233.
3. E.R. Vance, MRS Bulletin, **XIX** (12), 28 (1994).
4. D.A. Sverjensky, Nature, **358**, 310 (1992).
5. H. Xu and Y. Wang, J. Nucl. Mater., **275**, 216 (1999).
6. H. Xu, Y. Wang, and L. Barton, J. Nucl. Mater., **273**, 343 (1999).
7. H. Xu and Y. Wang, Radiochim. Acta, **87**, 37 (1999).
8. R.L. Putnam, A. Navrotsky, B.F. Woodfield, J.L. Shapiro, R. Stevens, and J. Boerio-Goates, In *Scientific Basis for Nuclear Waste Management XXII*, Boston (Nov. 30-Dec. 4, 1998) edited by D.J. Wronkiewicz and J.H. Lee (Mater. Res. Soc. Symp. Proc., **556**, Warrendale, PA, 1999) pp. 11-18.
9. R.L. Putnam, A. Navrotsky, B.F. Woodfield, J. Boerio-Goates, and J.L. Shapiro, J. Chem. Thermodynamics, **31**, 229 (1999).
10. R.G. Berman, J. Petrology, **29**, 445 (1988).
11. R. Robie and B.S. Hemingway, *Thermodynamic Properties of Minerals and Related Substances at 298.15 K and 1 Bar (10^5 Pascals) Pressure and at Higher Temperatures*, Geological Survey Bulletin No. 2131 (U.S. Geological Survey, Denver, CO) 461 pp. (1992).
12. H. Xu and Y. Wang, In *Radioactive Waste Management and Environmental Remediation—ICEM99,* in press (1999).
13. R.L. Putnam (personal communication) (1999).

14. T.J. Wolery, *EQ3/6, A Software Package for Geochemical Modeling of Aqueous Systems (Version 7.0)*, Lawrence Livermore National Laboratory, Livermore, CA, Report UCRL-MA-110662 Pt. 1 (1992).
15. H.W. Nesbitt, G.M. Bancroft, W.S. Fyfe, S.N. Karkhanis, and A. Nishijima, Nature, **289**, 358-362 (1981).